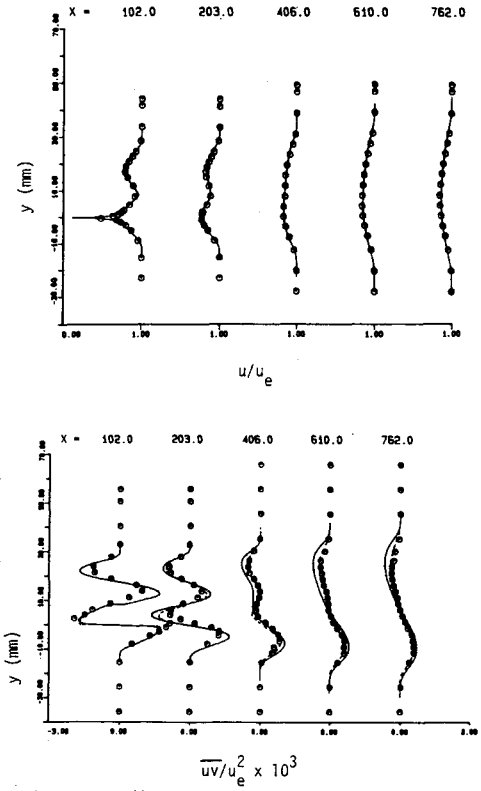

Fig. 3 Velocity profiles for overhang of 102.0 mm and gap of 19.0 mm.

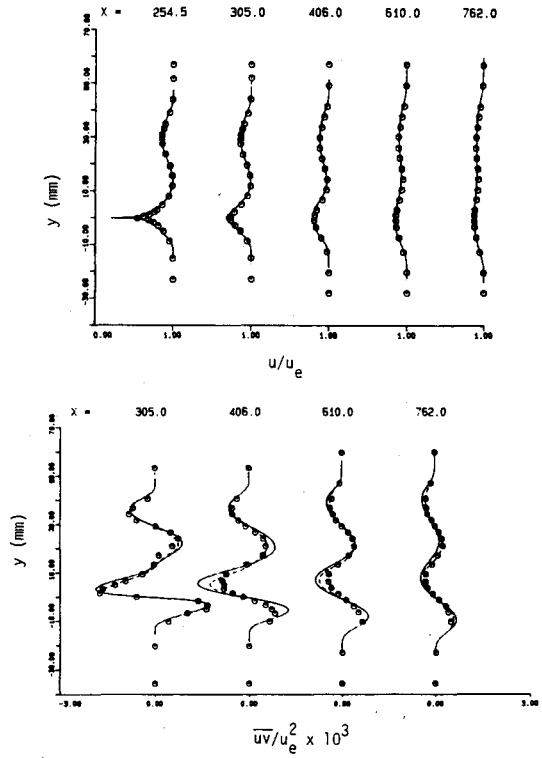

Fig. 4 Velocity profiles for overhang of 254.0 mm and gap of 19.0 mm.

Here x_{te} corresponds to the trailing edge, δ_{te} denotes the boundary-layer thickness at x_{te}, and ϵ_W represents the eddy viscosity of the far wake given by the maximum of ϵ_w, L and ϵ_w, U defined by

$$\epsilon_{w,L} = 0.064 \int_{-\infty}^{y_{\min}} (u_{e,L} - u)\, dy, \quad \epsilon_{w,U} = 0.064 \int_{y_{\min}}^{\infty} (u_{e,U} - u)\, dy$$

Here the subscript L and U denote the lower and upper wakes, respectively, and $y_{\min}$ corresponds to the normal distance where $u = u_{\min}$.

The eddy-viscosity expression for the interactive region between the two wakes is similar to that given by Eq. (1) provided that we replace ϵ_{te} with ϵ_{mg} and B_1 with B_2 defined by $B_2 = (x - x_{mg})/20\delta_{mg}$. Here x_{mg} corresponds to the distance where merging takes place, and δ_{mg} and ϵ_{mg} denote the boundary-layer thickness and the eddy viscosity calculated from Eq. (1) at that location, respectively. The merging location is defined to be the edge of the boundary layer (at $0.995u_e$) of two adjacent inner wakes which cross over.

Results and Conclusion

The experiments of Nakayama et al.[5] correspond to turbulent wall boundary layers on the two plates of Fig. 1. A sample of the results is shown on Figs. 2–4 with symbols representing experimental data, solid lines the algebraic turbulence model, and dashed lines the transport model.

Figure 2 represents the case of zero overhang and displays the poorest agreement between measured and calculated profiles of velocity in the near field, due to the confined nature of the flow and the need to adjust the turbulence model to deal with this arrangement. The results of the two models are virtually identical and the agreement with experiment improves with downstream distance. Figures 3 and 4 correspond to flows with two values of the overhang distance and show that the results obtained with the two models are in excellent agreement with experiment.

The results allow the same conclusion to be drawn for multiple wakes as Cebeci et al.[1] and Chang et al.[2] reported for wall boundary layers and single wakes. The two turbulence models provide essentially the same results and the use of the transport model has a cost penalty, in terms of computer run time, of a factor of three.

References

[1]Cebeci, T., Chang, K. C., Li. C., and Whitelaw, J. H., "Turbulent Models for Wall Boundary Layers," *AIAA Journal,* Vol. 24, March 1986, pp. 359–360.

[2]Chang. K. C., Bui, M. N., Cebeci, T., and Whitelaw, J. H., "The Calculation of Turbulent Wakes." *AIAA Journal,* Vol. 24, Feb. 1986, p. 200.

[3]Cebeci, T., and Smith, A. M. O., *Analysis of Turbulent Boundary Layers,* Academic, New York, 1974, Chap. 6.

[4]Hanjalic, K., and Launder, B. E., "Sensitizing the Dissipation Equation to Irrotational Strains" *Journal of Fluids Enqineerinq,* Vol. 102, March 1980, pp. 34–50.

[5]Nakayama, A., Kreplin, H.-P., and Liu, B., "Measurement of Wake/Wake Interactions in Zero Pressure-Gradient Flow," California State Univ., Long Beach, CA, Rept. ME-85-2, 1985.

[6]Cebeci, T., and Bradshaw, P., *Physical and Computational Aspects of Convective Heat Transfer,* Springer-Verlag, New York, 1988, Chap. 13.

Magnetization-Vector Analogy as a Reformulation of the Equations of Fluid Dynamics

Paolo Luchini*
University of Naples, Naples, Italy

Introduction

SEVERAL numerical methods of solving the incompressible Euler and Navier-Stokes equations in two dimensions

Received Oct. 4, 1989, revision received Jan. 18, 1990.

*Staff Research Scientist, Istituto di Gasdinamica, Facoltà di Ingegneria.

adopt a streamfunction-vorticity formulation, thus avoiding the difficulties associated with the implicit constraint of zero divergence imposed on the velocity field and the closely related calculation of pressure. Typical examples are lumped-vortex schemes and finite difference, finite element, or spectral methods based on the ψ-ζ formulation. The extension of these methods to three dimensions, however, has not been very successful because vorticity is a vector in three dimensions and, therefore, causes an increase of the number of unknowns with respect to the pressure it replaces, but even more because the three-dimensional vorticity field is subject to the same constraint of zero divergence, which was to be avoided in the first place.

Lumped-Vortex Formulations

Let us consider, in particular, lumped-vortex formulations, a very recent and detailed review of which has been given by Sarpkaya.[1] In two dimensions, the archetype of all lumped-vortex formulations is obtained by assuming a scalar vorticity field of the form

$$\zeta = \sum_{i=1}^{N} \zeta_i \delta[\boldsymbol{x} - \boldsymbol{x}_i(t)] \tag{1}$$

The Euler equations exactly reduce to the ordinary differential equations $d\boldsymbol{x}_i/dt = \boldsymbol{V}_i$ with ζ_i constant and the velocity field $\boldsymbol{V}$ given, in free space, by the Biot-Savart integral of magnetostatic theory. As is well known, such exactness is illusory because the singular behavior of velocity at the position of the vortices themselves needs to be smoothed out. In doing so, approximations are introduced, but, nevertheless, the lumped-vortex formulation is appealing for the calculation of unsteady inviscid flows in unbounded regions containing small vortical regions[2] or for the direct simulation of turbulence.[3] Generalizations to viscous flow[4] and to heat and mass transfer[5] have also been developed.

In three dimensions, the obvious extension of Eq. (1) is

$$\boldsymbol{\omega} = \sum_{i=1}^{N} \boldsymbol{\omega}_i \delta[\boldsymbol{r} - \boldsymbol{r}_i(t)] \tag{2}$$

However, there are several added difficulties that were not present in the two-dimensional case. Computationally, these are that ω_i is no longer a constant and must be calculated by solving its own evolution equation and the three-dimensional Biot-Savart integral involves vector quantities and, therefore, three scalar integrals. Conceptually, there is the deeper objection that Eq. (2) does not define a solenoidal (zero-divergence) vorticity field, and this property can only be ensured in some mean sense by choosing appropriate initial conditions; although the exact vorticity transport equation is such that an initially solenoidal vorticity field will remain, and so there is no guarantee that numerical errors shall not accumulate to the point of making significant sources or drains appear.

The last comment leads us to the main point of this Note, which is to suggest that the most convenient variable for describing three-dimensional vortices is not vorticity but a related concept that corresponds, in the magnetostatic analogy, to the magnetization vector.

Magnetostatic Analogy

The magnetostatic analogy from which the Biot-Savart law is borrowed originates from the simple observation that the pair of equations div $\boldsymbol{V} = 0$, curl $\boldsymbol{V} = -\boldsymbol{\omega}$ relating velocity and vorticity is identical to the equations div $\boldsymbol{B} = 0$, curl $\boldsymbol{B} = \boldsymbol{J}$ of magnetostatics. In magnetostatics, however, it is well known that the current density $\boldsymbol{J}$ is not the only, nor necessarily the most convenient, way of describing the source of a magnetic field. An alternative description is offered by the magnetization vector $\boldsymbol{M}$, which is the density of magnetic dipoles rather than of electric currents. Mathematically, the relation between $\boldsymbol{M}$ and $\boldsymbol{J}$ is, apart from dimensional constants depending on the system of units, which we need not be concerned with, curl $\boldsymbol{M} = \boldsymbol{J}$ (which does not imply that $\boldsymbol{B} = \boldsymbol{M}$ because div $\boldsymbol{M} \neq 0$). The calculation of $\boldsymbol{B}$ from $\boldsymbol{M}$ is simply achieved by observing that the vector $\boldsymbol{B} - \boldsymbol{M}$, i.e., the magnetic $\boldsymbol{H}$ vector, is irrotational and, therefore, may be expressed as $-\nabla\varphi$ (φ being the scalar potential of magnetostatics). The scalar φ may, in turn, be calculated by solving the Laplace equation $\Delta_2\varphi = \text{div } \boldsymbol{M}$. Notice that wherever $\boldsymbol{M} = 0$ (e.g., outside magnets), $\boldsymbol{B} = -\nabla\varphi$.

What is the fluid dynamic analog of a magnetic dipole? It turns out to be a very familiar concept: a ring vortex. This may be understood by remembering that a magnetic dipole is equivalent to an infinitesimal current loop. Since current density corresponds to vorticity, a fluid-dynamic magnetic dipole is an infinitesimal vorticity loop, which is an infinitesimal ring vortex. As ring vortices are known to be quite persistent structures in a three-dimensional field, an approximate description in terms of a finite number of infinitesimal ring vortices seems even physically more appealing than one in terms of infinitesimal lumps of vorticity. Let us now see how such a model can be formulated.

Instead of Eq. (2), we assume

$$\boldsymbol{M} = \sum_{i=1}^{N} \boldsymbol{m}_i \delta[\boldsymbol{r} - \boldsymbol{r}_i(t)] \tag{3}$$

that is,

$$\boldsymbol{\omega} = -\text{curl } \boldsymbol{M} = \sum_{i=1}^{N} \boldsymbol{m}_i \wedge \nabla\delta\,[\boldsymbol{r} - \boldsymbol{r}_i(t)] \tag{4}$$

Notice that for $N \to \infty$ any solenoidal vector field may be represented in the distribution sense by Eq. (4) as well as by Eq. (2).

In order to obtain the differential equations for $\boldsymbol{M}$ and subsequently $\boldsymbol{m}_i$ and $\boldsymbol{r}_i$, let us put $\boldsymbol{V} = \boldsymbol{M} - \nabla\varphi$ (which is the analog of $\boldsymbol{B} = \boldsymbol{M} - \nabla\varphi$) in the Euler momentum equation:

$$\frac{\partial}{\partial t}(\boldsymbol{M} - \nabla\varphi) + (\boldsymbol{M} - \nabla\varphi) \cdot \nabla\,(\boldsymbol{M} - \nabla\rho) + \nabla p = 0 \tag{5}$$

The terms in Eq. (5) may be regrouped, actually in more than one way, into a part that is zero for $\boldsymbol{M}$ zero and a part that is the gradient of a scalar. Two such regroupings are

$$\boldsymbol{M}_t + \boldsymbol{V} \cdot \nabla\boldsymbol{M} - \nabla\nabla\varphi \cdot \boldsymbol{M} + \nabla[p - \varphi_t + (\nabla\varphi)^2/2] = 0 \tag{6a}$$

$$\boldsymbol{M}_t + \boldsymbol{V} \cdot \nabla\boldsymbol{M} - \nabla\boldsymbol{M} \cdot \boldsymbol{V} + \nabla[p - \varphi_t + \boldsymbol{V}^2/2] = 0 \tag{6b}$$

Now we can exploit the extra degree of freedom gained by having replaced three unknowns by four (the three components of $\boldsymbol{V}$ by φ plus the three components of $\boldsymbol{M}$) to set the scalar expression in square brackets equal to zero. Doing so, for instance, in Eq. (6a), leaves us with an equation for $\boldsymbol{M}$, in which the pressure no longer appears, namely,

$$\boldsymbol{M}_t + \boldsymbol{V} \cdot \nabla\boldsymbol{M} - \nabla\nabla\varphi \cdot \boldsymbol{M} = 0 \tag{7}$$

plus an explicit expression of the pressure, given by

$$p = \varphi_t - (\nabla\varphi)^2/2 \tag{8}$$

Equation (7) forms a system with the continuity equation

$$\Delta_2\varphi = \text{div } \boldsymbol{M} \tag{9}$$

Equations (7) and (9) are, in a sense, analogous to the equations for vorticity and streamfunction; however, they do not increase the number of unknowns with respect to the velocity-pressure formulation because φ is a scalar, and the $\boldsymbol{M}$ field is not subject to any additional constraint of zero divergence as vorticity is. As an added benefit, the present method furnishes the explicit expression [Eq. (8)] for the pressure, whereas in

the usual vorticity-streamfunction formulation the calculation of pressure is a nontrivial problem.

Notice that the possibility of deriving an equation for M in more than one way stems from the nonunique mathematical definition of M according to the equation curl $M = -\omega$. It does not cause any contradiction as long as a single choice is consistently used because all of these different N correspond to the same velocity field. A similar situation occurs in magnetism as well, where M is left partly undefined by the relation curl $M = J$, and different magnetization vectors may appear in physically equivalent descriptions of the same problem. As long as a formulation is chosen in which the equation for M [e.g., Eq. (7)] is satisfied for M identically zero [which means, in particular, that any term not multiplied by M in Eq. (5) has been confined to the gradient part], M will share with vorticity the property of remaining nonzero only in the vortical region, if it is initially so, and the irrotational regions of the velocity field will be described by the potential φ only.

Extension of the foregoing concepts to the viscous Navier-Stokes equations is straightforward; it only requires the addition of a term $\nu\Delta_2 M$ to the right side of Eq. (7) and a term $-\nu\Delta_2\varphi$ to the right side of Eq. (8).

Obtaining a lumped-ring-vortex formulation from the previous equations is formally easy: one need only insert Eq. (3) into Eq. (7). Doing so yields the equations

$$\frac{d\boldsymbol{r}_i}{dt} = \boldsymbol{V}(\boldsymbol{r}_i); \qquad \frac{d\boldsymbol{m}_i}{dt} = \nabla\nabla\varphi(\boldsymbol{r}_i)\cdot\boldsymbol{m}_i \tag{10}$$

which describe the convection and stretching of the ring vortices and, just as in the two-dimensional case, are exact, at least until the necessary smoothing is introduced. These are similar to the equations that govern infinitesimal lumps of vorticity. The important difference is that the M field is unconstrained and need not be solenoidal. The vectorial Biot-Savart integral is replaced by the faster-to-compute scalar integral, which represents the scalar potential of a magnetic dipole distribution:

$$\varphi(\boldsymbol{r}) = \int \nabla'\left(\frac{1}{4\pi R}\right)\cdot\boldsymbol{M}(\boldsymbol{r}')\,d^3\boldsymbol{r}' \tag{11}$$

(where ∇' denotes the gradient with respect to r' and $R = |r - r'|$). We may also remark that, once the velocity field is recovered from Eq. (11) as $V = M - \nabla\varphi$, it decays with distance from the source point as R^{-3}, whereas the one in the three-dimensional Biot-Savart law only as R^{-2}, thus affording greater possibilities of neglecting, in an approximation context, the influence of far vortices.

Results and Discussion

On the negative side, it must be said that the smoothing necessary to eliminate the singularity from Eq. (11) and transform Eqs. (10) and (11) into a workable numerical scheme still presents nontrivial problems similar to those encountered by the vorticity formulation. The basic technique remains the same: to replace the infinitesimal ring vortex represented by a δ function in Eq. (3) by an extended, three-dimensional, magnetization blob. The shape and size of this blob, however, must be chosen with care, and criteria must be devised for merging and splitting blobs when they become too small or too large with respect to the scale of variation of the velocity field that they generate. In fact, blob size may turn out to be even more critical than in other formulations because of the self-interaction of ring vortices, which propels them about with a speed inversely related to size. It remains true for a lumped-vortex numerical scheme based on the magnetization formulation that, as remarked by Sarpkaya[1] for previous lumped-vortex schemes, the choice of the smoothing method constitutes its most delicate numerical aspect.

On the other hand, the integro-differential equations [Eqs. (7) and (11)] [the latter being nothing else than the analytical solution of Eq. (9) in free space] are a quite general reformulation of the Euler (or Navier-Stokes) equations and their use in computational fluid dynamics is by no means limited to lumped-vortex formulations. In this context, it is interesting to discuss the boundary conditions that must be coupled to these equations when solid bodies are present. Again, the replacement of the three components of V by four new unknowns gives us some freedom. In particular, we may choose to use Eq. (11) as is, even when walls are present, and solve Eq. (7) with conditions specifying that the normal component of $M - \nabla\varphi$ should vanish at a wall. This is an implicit condition involving values of M in the whole field, but may be convenient in lumped-vortex formulations as it corresponds to the replacement of walls by bound vortices. Alternatively, we may choose to solve Eq. (9) with boundary conditions specifying zero normal velocity at the walls; the normal component of M at a wall then becomes arbitrary and may, for instance, be set equal to zero, thus giving an explicit boundary condition. In the extension to the Navier-Stokes equations, when all three velocity components must vanish at a wall, both choices yield implicit boundary conditions; the second choice, however, being explicit for the Euler equations, is preferable because one can expect that only calculation points in the nearby boundary layer, where viscous effects are relevant, need be effectively involved.

Conclusion

Finally, let us observe that the classical two-step method by Chorin[6,7] that solves the time-dependent Navier-Stokes equations in primitive velocity-pressure variables may be obtained as a special case of the magnetization approach. Indeed, we still haven't discussed the conditions to be given to Eqs. (7-9) at initial time. Again, some freedom is involved, and we may arbitrarily choose the initial value of the potential φ, thereafter determining the initial value of M as $V(t_0) + \nabla\varphi$ [Eq. (11) will then be automatically satisfied provided the initial V field is solenoidal]. Different choices will give us different M fields at subsequent times, which, however, all correspond to the same velocity field, much in the same way as different potential gauges in electromagnetic theory correspond to the same field. The most obvious (but not necessarily the most convenient) choice is to set $\varphi = 0$ initially, so that $M(t_0) = V(t_0)$. If Eq. (7) is then discretized in time, it will be seen to correspond to Chorin's first step, in which the evolution of velocity is calculated as though pressure were absent; Eqs. (9) and (11) will then correspond to Chorin's second step when a potential correction is applied in order to recover the solenoidal character of the velocity field. If we now reset $M = V$, rather than continuing the solution of Eq. (7) with the value of M just obtained, we shall have Chorin's method. Notice, however, that in an open-space flow in which vorticity is only present in a small region this may not be a wise thing to do; it is much more convenient to retain M, which, just as vorticity, is only nonzero in a small region, as the main unknown, and restrict the calculation domain to the vortical region only.

References

[1]Sarpkaya, T, "Computational Methods with Vortices – The 1988 Freeman Scholar Lecture," *Journal of Fluids Engineering,* Vol. 111, No. 1, 1989, pp. 5–52.

[2]Tryggvason, G., "Simulation of Vortex Sheet Roll-up by Vortex Methods," *Journal of Computational Physics,* Vol. 80, No. 1, 1989, pp. 1–16.

[3]Chein, R., and Chung, J. N., "Discrete-Vortex Simulation of Flow over Inclined and Normal Plates," *Computers and Fluids,* Vol. 16, No. 4, 1988, pp. 405–428.

[4]Choquin, J. B., and Huberson, S., "Particles Simulation of Viscous Flow," *Computers and Fluids,* Vol. 17, No. 2, 1989, pp. 397–410.

[5]Ghoniem, A. F., and Givi, P., "Lagrangian Simulation of a Reacting Mixing Layer at Low Heat Release," *AIAA Journal,* Vol. 26, No. 6, 1988, pp. 690–697.

[6]Chorin, A. J., "Numerical Solution of the Navier-Stokes Equations," *Mathematics of Computation*, Vol. 22, No. 86, 1968, pp. 745-762.

[7]Chorin, A. J., "On the Convergence of Discrete Approximations to the Navier-Stokes Equations," *Mathematics of Computation*, Vol. 23, No. 90, 1969, pp. 341-353.

Expressions for k and ϵ Near Walls

Y.-H. Hwang* and T.-M. Liou†
National Tsing Hua University, Taiwan, Republic of China

Introduction

THE so-called wall functions have been widely used by the recent turbulence closure models in the prediction of wall-bounded shear flows. Certain distributions, e.g., the local heat transfer coefficient, are especially sensitive to the near-wall model. Consequently, a brief survey of previous formulas describing the near-wall distributions of the turbulence parameters would be worthwhile.

The logarithmic law for the mean-velocity distribution was derived by various researchers,[1,2] based on different hypotheses and highly supported by the experimental data.[3] Spalding[4] simplified the turbulent kinetic energy equation under three different cases, obtaining $k \sim y^{m_1}$ for the zero-shear layer, $k \sim$ constant for the constant-shear layer, and $k \sim y$ for the linear-shear layer. However, these solutions cannot be applied to the pipe axis or the edge of the boundary layer. In addition, Spalding did not provide solutions for ϵ, dissipation rate of the turbulent kinetic energy. Launder and Spalding[5] deduced $k = C_\mu^{-1/2}\tau_w/\rho$, $\epsilon \sim k^{3/2}/y$ and, consequently, the most widely used wall functions by an analysis of experimental data and by the rationale of the order of magnitude. The main assumption for the wall functions is the presence of an equilibrium layer where the generation and dissipation of k are in balance. No corresponding expressions relevant to the viscous sublayer and the outer layer were provided. El-Hawary and Nicoll[6] used empirical relations—$k = q(y^+/26)^{m_2}$ for $y^+ \le 26$, $k = q$ for $26 < y^+ < 70$, and $k = q(1 - y/\delta)$ for $y^+ > 70$—to represent the available experimental data in the entire boundary layer. Chieng and Launder[7] proposed a parabolic variation of k within the viscous sublayer, $k = k_v(y/y_v)^2$, based on a Taylor series expansion of the fluctuating velocity at the wall. The ϵ is not zero in the viscous sublayer, and has been shown by Pope and Whitelaw[8] to be constant equal to $2\nu_\ell(\partial k^{1/2}/y)^2$. By series expansion, Launder[9] and Patel et al.[10] also proposed $\epsilon = \epsilon_w + C_\epsilon y^2$ in the viscous sublayer, with ϵ_w and C_ϵ determined from experimental data. Recently, Wilcox[11] used the perturbation method to deduce $k \sim y^{3.23}$ and the specific dissipation rate $\omega = 6\nu_\ell/(\beta y^2)$ in the viscous sublayer.

The above literature survey reveals that most of the formulas for k and ϵ distributions close to the wall are either empirical or approximate, with the use of series expansion to represent the experimental data within a certain layer. There is lack of analytic expressions for both k and ϵ distributions in the near-wall region. The purpose of this paper is, therefore, to propose a set of algebraic relationships that attempt to model the near wall region of a turbulent boundary layer for the distributions of k and subsequent ϵ. The resulting expressions will be examined by the previous measurements and compared with previous derivations.

Received June 26, 1989; revision received March 3, 1990; accepted for publication April 16, 1990.

*Graduate Student, Power Mechanical Engineering Department.
†Professor, Power Mechanical Engineering Department.
Address correspondence to Prof. Tong-Miin Liou, Dept. of Power Mechanical Engineering, National Tsing Hua University, Hsin-Chu, Taiwan 30043, R.O.C.

Analysis

The governing equation of k for the boundary layer or the fully developed turbulent pipe flows can be simplified as follows:

$$\frac{d}{dy}\left[\left(\mu_\ell + \frac{\mu_t}{\sigma_k}\right)\frac{dk}{dy}\right] - \rho\overline{uv} - \rho\epsilon = 0 \tag{1}$$

In the following analysis, three turbulent models—$k-\epsilon$, $k-L$, and $k-\omega$—will be adopted to derive the distributions of k and ϵ in the near-wall region.

Analysis Based on the $k-\epsilon$ Model

In the fully turbulent region close to the wall, $\mu_\ell \ll \mu_t$, the Prandtl's mixing-length and the logarithmic mean-velocity profile give $\mu_t = \rho\kappa y U_\tau$. For $k-\epsilon$ model, one has $\epsilon = C_\mu \rho k^2/\mu_t$. If the Boussinesq's eddy viscosity concept is further adopted, Eq. (1) reduces to an autonomous equation

$$\frac{d}{dy^+}\left(y^+\frac{dk^*}{dy^+}\right) + \frac{\sigma_k C_\mu^{1/2}}{\kappa^2 y^+}(1 - k^{*2}) = 0 \tag{2}$$

with $k^* = C_\mu^{1/2}k/U_\tau^2$ and $y^+ = \rho U_\tau y/\mu_t$, and may be integrated to obtain

$$k^* = 3\left[\frac{(A_\pm y^+)^{\pm h^*} - 1}{(A_\pm y^+)^{\pm h^*} + 1}\right]^2 - 2 \tag{3}$$

for the inner branch (A_+; $+h^*$; $dk^*/dy^+ > 0$) and the outer branch (A_-; $-h^*$; $dk^*/dy^+ < 0$) of the equilibrium layer, respectively, where $h^* = (2\sigma_k)^{1/2}C_\mu^{1/4}/\kappa$. Note that the physical conditions, $k^* = 1$ and $dk^*/dy^+ = 0$, which result from assuming the presence of an equilibrium layer,[10] have been applied to determine the integration constants. The further constants A_+ and A_- can be determined by matching Eq. (3) with the solution for the viscous sublayer ($y_v^+ = 5.0$)

$$k^* = a_c C_\mu^{1/2} y^{+2} \tag{4}$$

and with $k^* = 0$[6] at the pipe axis or at the edge of the boundary layer, respectively. In deriving Eq. (4), the terms associated with μ_t and $-\rho\overline{uv}$ in Eq. (1) have been neglected and $\epsilon = 2\nu_\ell(dk^{1/2}/dy)^2$, proposed by Chieng and Launder,[9] has been adopted. The wall condition $k^* = 0$ has also been used. The constant a_c has a mean value of 0.045, recommended by Derksen and Azad.[12] It may be noted that the solution in Eq. (4) has the same form as that derived by Chieng and Launder[9] with the use of Taylor series expansion.

A combination of $\mu_t = \rho k y U_\tau$, $\epsilon = C_\mu \rho k^2/\mu_t$, and $\epsilon^+ = \mu_t \epsilon/(\rho U_\tau^4)$ leads to

$$\epsilon^+ = \frac{k^{*2}}{\kappa y^+} \tag{5}$$

for the near-wall region, where k^* is given by Eq. (3). Very near the wall, Patel et al.[10] proposed the empirical expression $\epsilon = \epsilon_w + C_\epsilon y^2$ for the viscous sublayer, which can be expressed as

$$\epsilon^+ = 2a_c + a_\epsilon y^{+2} \tag{6}$$

by the use of $\epsilon = 2\nu_\ell(dk^{1/2}/dy)^2$ and Eq. (4). The continuity of ϵ requires that Eq. (5) be equal to Eq. (6); thus, a_ϵ is determined.

Additionally, the dissipation term of the k equation in the $k-\epsilon$ model is usually computed by the following integration:

$$\overline{\epsilon^+} = \int_0^{y^+} \epsilon^+ dy^+ = \frac{1}{\kappa}\ell n(y^+/y_v^+) \pm (2/3)^{1/2}\frac{1}{\sigma_k^{1/2}C_\mu^{1/4}} \times [(k^{*3} - 3k^* + 2)^{1/2} - (k_v^{*3} - 3k_v^* + 2)^{1/2}] + 2a_c^2 y_v^+ + \frac{1}{3}a_\epsilon y_v^{+3} \tag{7}$$